Graduate School of Oceanography Faculty Publications

Graduate School of Oceanography

2003

Influence of dust and sulfate aerosols on ocean color spectra and chlorophyll a concentrations derived from SeaWiFS off the U.S. east coast

Stephanie E. Schollaert
University of Rhode Island

James A. Yoder
University of Rhode Island, jimyoder@uri.edu

John E. O'Reilly

Douglas L. Hestphal

Follow this and additional works at: https://digitalcommons.uri.edu/gsofacpubs

Influence of dust and sulfate aerosols on ocean color spectra and chlorophyll a concentrations derived from SeaWiFS off the U.S. east coast

Influence of dust and sulfate aerosols on ocean color spectra and chlorophyll *a* concentrations derived from SeaWiFS off the U.S. east coast

Stephanie E. Schollaert and James A. Yoder

Graduate School of Oceanography, University of Rhode Island, Narragansett, Rhode Island, USA

John E. O'Reilly

Northeast Fisheries Center, Narragansett Laboratory, NOAA/NMFS, Narragansett, Rhode Island, USA

Douglas L. Westphal

Marine Meteorology Division, Naval Research Laboratory, Monterey, California, USA

[1] The influence of two dominant aerosol species on satellite ocean color retrievals is examined off the U.S. East Coast in the western Sargasso subtropical gyre. Waters of very low chlorophyll concentration have normalized water-leaving radiance (*nLw*) spectra highest in blue and decreasing monotonically with increasing wavelength. For water with chlorophyll concentrations less than 0.13 mg m^{-3} we compared the Sea-viewing Wide Field-of-view Sensor (SeaWiFS) *nLw* spectra for different aerosol conditions (clear, dust-dominated, and sulfate-dominated) over 1 year between March 1999 and March 2000. With appropriate atmospheric correction, satellite-derived *nLw* spectra should be insensitive to the presence of atmospheric aerosols, but we found the SeaWiFS spectra to be sensitive to the species and optical thickness of aerosols. The SeaWiFS bio-optical chlorophyll algorithms use $nLw(\lambda)/nLw(555)$ band ratios (where λ = 443, 490, or 510 nm): any biases in the band ratios result in incorrect chlorophyll concentration estimates. When aerosols were negligible, *nLw* spectra were consistent with in situ reference data between 443 and 510 nm. With increasing aerosol optical thickness during dust events, most common during summer, the *nLw* spectra were lowered between 412 and 510 nm, decreasing $nLw(\lambda)/nLw(555)$ band ratios and resulting in artificially high chlorophyll *a* estimates. Sulfate-dominated pixels were associated with elevated *nLw* spectra between 412 and 555 nm. Increasing sulfate optical thickness corresponded to decreases of the bio-optical band ratios because of the increase at 555 nm, which also biased the chlorophyll *a* estimates high. The effect of sulfate upon ocean color retrievals is more problematic than dust off the U.S. east coast because of the nearly constant presence of sulfate along with commonly colocated pollutant aerosols that confound atmospheric correction algorithms. *INDEX TERMS:* 4847 Oceanography: Biological and Chemical: Optics; 4275 Oceanography: General: Remote sensing and electromagnetic processes (0689); 4548 Oceanography: Physical: Ocean fog and aerosols; 0305 Atmospheric Composition and Structure: Aerosols and particles (0345, 4801); 0394 Atmospheric Composition and Structure: Instruments and techniques; *KEYWORDS:* SeaWiFS, atmospheric correction, chlorophyll *a*, aerosols, dust, sulfate

1. Introduction

[2] An ocean color satellite sensor such as the Sea-viewing Wide Field-of-view Sensor (SeaWiFS) receives about 90% of its signal from the atmosphere while only about 10% comes from the ocean [*Wang*, 1999]. In order to derive the portion of radiance leaving the water the atmospheric contribution must be estimated and subtracted from the total radiance recorded at the top of the atmosphere. The atmospheric contribution is due to Rayleigh and aerosol scattering. Rayleigh scattering is well understood and easily estimated. Aerosol scattering has proven more problematic. Satellite remote sensing of the ocean requires good information on the radiative characteristics of the intervening aerosols, particularly their impact on backscattering. Estab-
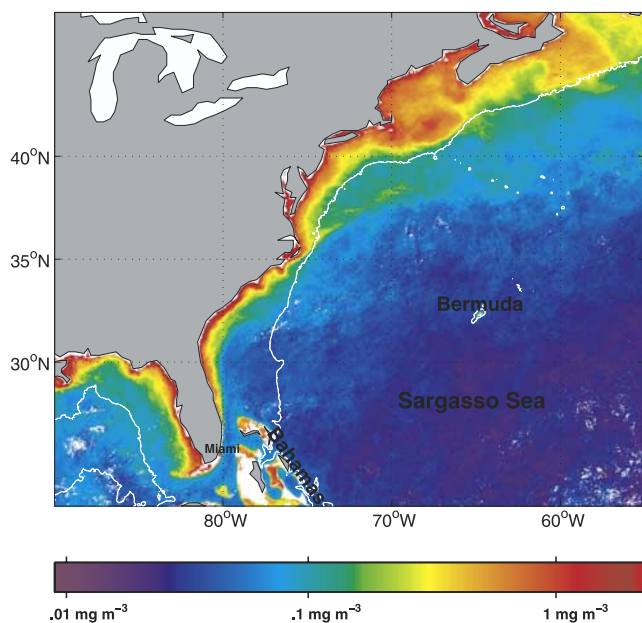
Figure 1. SeaWiFS chlorophyll *a* composite off the U.S. east coast from July to December, 1999. Land is masked grey the white contour adjacent to the coast delineates the 2000 m isobath.

lishment of a climatology of these characteristics for remote sensing and climate monitoring has been a major objective of the scientific community, in particular, the International Aerosol Climatology Project, for the past several decades. New space-borne instruments will soon yield a more detailed characterization of the aerosols (aerosol optical depth, size distribution, refractive index, and perhaps shape of the particles [*Antoine and Morel*, 2000]). For processing SeaWiFS imagery the aerosol contribution is determined at near-infrared wavelengths where the water is assumed to be totally absorbing. For the shorter visible wavelengths the aerosol contribution must be estimated by extrapolation based on various models of aerosol composition, vertical distribution, and spectral shape [*Gordon*, 1997]. Off the U.S. east coast the tropospheric aerosol population is complex and variable. Non−sea salt sulfate from upwind urban sources is commonly present; mineral dust from continental sources is present episodically; and other aerosols such as sea salt, smoke, and nitrate are also present at various times. Here we characterize the effects of the two most common optically active aerosols, sulfate and dust [*Li et al.*, 1996], on the SeaWiFS bands used to derive chlorophyll *a* estimates.

[3] For the lowest chlorophyll region off the U.S. east coast, the Sargasso Sea, we examined SeaWiFS water-leaving radiance (*nLw*) spectra during different atmospheric conditions: clear, dust aerosol−dominated, and sulfate aerosol−dominated. Case I waters are classified as those for which phytoplankton and their covarying derivative products play a dominant role in determining the optical properties of the ocean, such that backscattered light is correlated with chlorophyll *a* concentration [*Gordon and Morel*, 1983]. The Sargasso approximates case I water more closely than any other area off the U.S. east coast. Much of what is

known about the natural seasonal variability of chlorophyll concentrations in this region comes from the Bermuda Atlantic Time-series Study (BATS). Near-surface in situ chlorophyll *a* concentrations measured at BATS during the time frame of this study revealed a tenfold variation, with the minimum in August around 0.03 mg m^{-3} and the maximum in March around 0.35 mg m^{-3}. On the basis of the BATS observations, *Siegel and Michaels* [1996] concluded that seasonal variations of optical properties within the clear Sargasso Sea do not necessarily covary with chlorophyll but rather with detrital particulate and color dissolved organic materials. We limit our study to those pixels whose chlorophyll concentrations are less than 0.13 mg m^{-3} and focus on July and August when low-chlorophyll pixels were in greatest abundance in each scene. Limiting the range of chlorophyll values going into our comparisons and looking over many months of imagery is also a way to minimize the number of other variables that could simultaneously bias SeaWiFS *nLw* retrievals, such as the unaccounted for dependence of SeaWiFS *nLw* upon the bidirectional reflectance of the ocean [*Morel and Gentili*, 1993], which depends upon the satellite view angle relative to the solar zenith angle and changes each day as the satellite drifts westward. On average, SeaWiFS covers this region with a near-nadir view every 3 days. Any 3 day sequence covering the same area has different solar satellite viewing geometries that could potentially affect the *nLw* spectra and lead to apparent changes in chlorophyll concentrations. Yet another possible source for systematic error arises from the fact that SeaWiFS ocean color data are vicariously calibrated at a single point on Earth using comparisons with the water-leaving radiances from the Marine Optical Buoy (MOBY) off of Hawaii. A thorough review of the calibration used to process SeaWiFS data since the third reprocessing has ascertained that *nLw* at 412, 443, and 490 nm have been underestimated by 16, 8, and 6%, respectively. Increasing the MOBY gains accordingly has resulted in a 7% decrease in chlorophyll concentrations (http://seawifs.gsfc.nasa.gov/
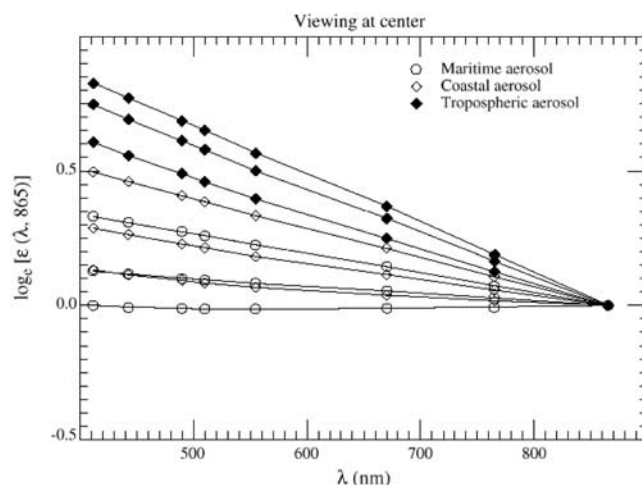

Figure 2. From *Gordon* [1997's Figure 3a], $\epsilon(\lambda, 865)$ for nadir viewing with $\theta_0 = 60°$ for the maritime, coastal, and tropospheric aerosol models. For each model the relative humidity values are 50, 80, and 98% from the upper to the lower curves.
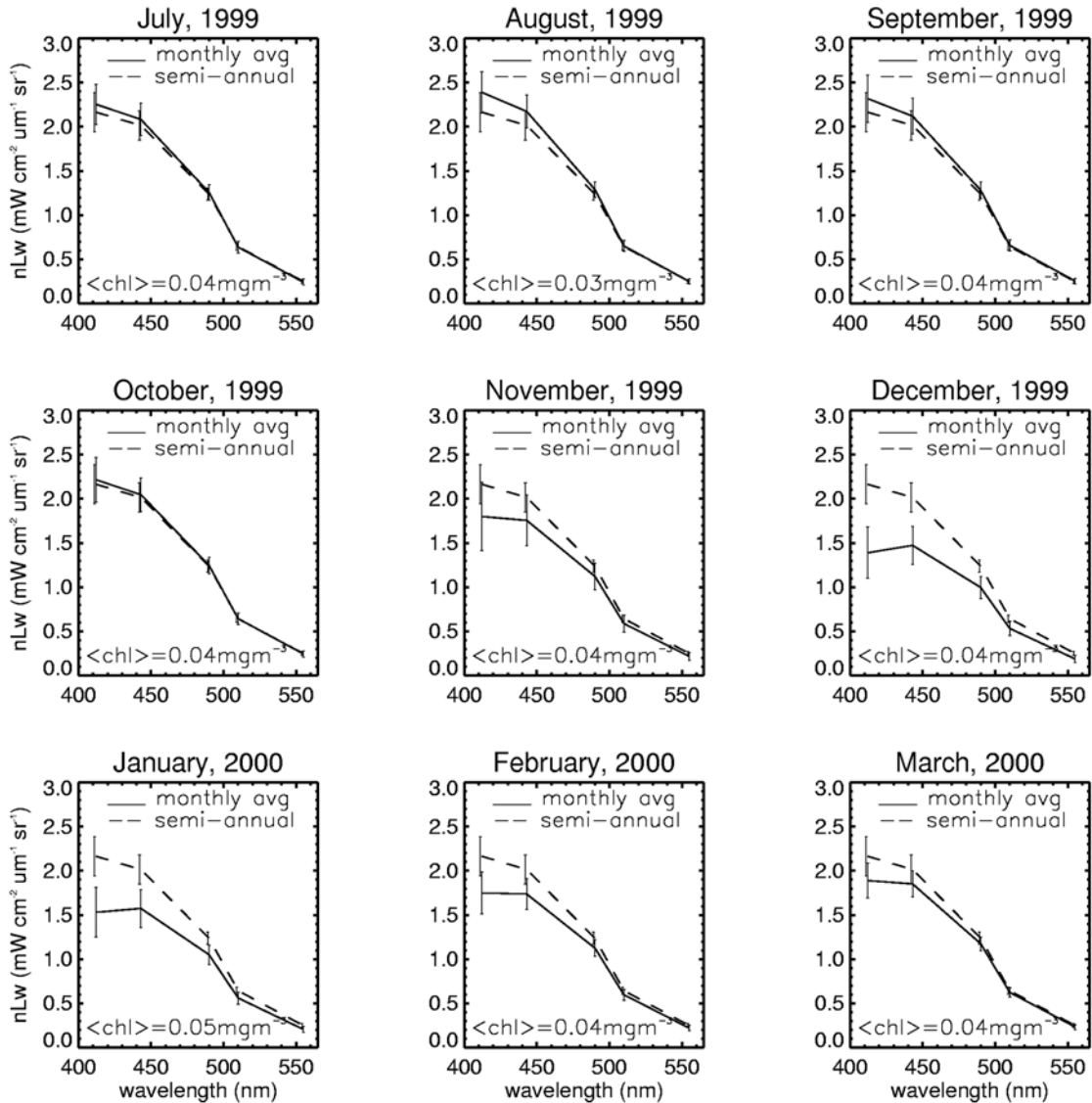
Figure 3. Monthly clear-sky (tau-865 < 0.05) chl$_{lowest}$ average $nLw(\lambda)$ spectra with the semiannual average (calculated from July to December 1999) superimposed on each month for orientation.

SEAWIFS/RECAL/Repro4). Another regional study within the California Current found an underestimation of Sea-WiFS nLw at 490 nm for high chlorophyll concentrations (3–5 mg m^{-3}), which they attributed to atmospheric correction problems [*Kahru and Mitchell*, 1999]. Similarly, we find an atmospheric correction problem off the U.S. east coast, which is more problematic than the other variables that bias the SeaWiFS nLw retrievals and is attributable to the aerosols common in the area. The effects of sulfate and dust are examined in detail because these two may pose the greatest challenge to atmospheric correction algorithms used in deriving ocean color fields.

2. Methods

[4] In oligotrophic water the water-leaving radiance spectra have long been modeled as a simple function of chlorophyll a concentration with minimal variability [*Morel*, 1988]. Normalized water-leaving radiance is approxi-

mately the radiance that would exit the ocean's surface when the Sun is at zenith [*Gordon*, 1997], derived from satellite measurements by

$$nLw(\lambda) = \frac{Lw(\lambda)}{\cos\theta \cdot \exp\left\{-\left[\frac{\tau_R(\lambda)}{2} + \tau_{oz}(\lambda)\right]\left(\frac{1}{\cos\theta}\right)\right\}},$$

where satellite-measured $Lw(\lambda)$ is the radiance backscattered out of the water toward the zenith at wavelength λ, θ is the solar zenith angle, and τ_R and τ_{oz} are the optical thicknesses of the atmosphere associated with Rayleigh scattering and ozone absorption, respectively. The nLw spectra associated with the dust and sulfate aerosol species were compared with the average clear-sky spectra to determine whether any persistent aerosol species-dependent bias exists. Improperly correcting for the atmosphere would result in persistently incorrect spectra and thus incorrect chlorophyll a concentration estimates. The SeaWiFS aerosol
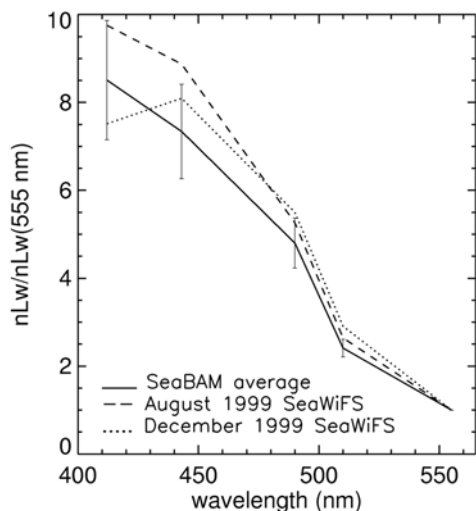
Figure 4. SeaBAM chl$_{lowest}$$nLw(\lambda)/nLw(555)$ spectrum (solid line) plotted with the SeaWiFS monthly clear-sky (tau-865 < 0.05) chl$_{lowest}$ average spectra for August (dashed line) and December (dotted line) 1999.

optical thickness at 865 nm, or tau-865, was used to determine the presence or absence of aerosols and to quantify their effect (i.e., how much aerosol present). The Navy Aerosol Analysis and Prediction System (NAAPS) global model was used to characterize dominant aerosol species as either mineral dust or non−sea salt sulfate. For comparison with the SeaWiFS nLw spectra we used in situ data from 1174 highest-quality global chlorophyll and associated spectral measurements, which had been carefully selected during the SeaWiFS Bio-Optical Algorithm Mini-Workshop (SeaBAM) for bio-optical algorithm tuning and evaluation [*O'Reilly et al.*, 1998] and are considered well representative of case I waters.

2.1. SeaWiFS Ocean Color Data

[5] SeaWiFS data were acquired as high-resolution picture transmission (HRPT) data downloaded at NASA Goddard Space Flight Center, Greenbelt, Maryland, and distributed by the Distributed Active Archive Center. The data were processed at the University of Rhode Island using the SeaWiFS processing and image analysis software package SeaDAS 4.0 [*Fu et al.*, 1998], also known as Reprocessing Version 3. From the level 1a data we generated level 2 products (nLw at five bands: 412, 443, 490, 510, and 555 nm; chlorophyll *a*; and tau-865) and remapped them to the east coast projection shown in Figure 1 at the highest resolution (1 km/pixel).

[6] Level 2 data were generated using the multiscattering aerosol correction scheme that uses 765 and 865 nm for aerosol model selection and up to 10 near-infrared iterations [*Siegel et al.*, 2000]. The standard SeaDAS thresholds and masks were used with the following modifications: solar zenith threshold was lowered to 70°, and the following flags were added to the mask: low $nLw(555)$, solar zenith angle, and stray light. The SeaWiFS aerosol lookup tables, generated from 12 aerosol models, are used to derive level 2 products [*Gordon*, 1997]. The 12 models are based upon four aerosol classes (oceanic, maritime, coastal, and tropospheric)

and varying relative humidity. The atmospheric correction scheme is based on the assumption that the strong absorption by water in the near infrared allows almost no backscattering, aside from Sun glint and whitecaps, so that after removing the Rayleigh contribution, reflectance observed at the top of the atmosphere may be attributed entirely to aerosols at these wavelengths. The ratio of the aerosol reflectance at 765 and 865 nm is then used to select a pair of aerosol models from 12 candidates (Figure 2) [from *Gordon*, 1997, Figure 3a]. The aerosol model pair gives the expected aerosol reflectances for the remainder of the spectrum. These aerosol reflectances are then subtracted from the Rayleigh-corrected top-of-the-atmosphere reflectances at each band to yield the water-leaving reflectances. Radiances are calculated through a simple conversion of the reflectances. These steps are done on each pixel without any input from adjacent pixels.

[7] Chlorophyll *a* concentrations were estimated within SeaDAS using the newest ocean color algorithm, OC4 [*O'Reilly et al.*, 2000], which became the SeaWiFS standard in May 2000. OC4 uses the logarithm of the maximum band ratio of $nLw(443)/nLw(555)$, $nLw(490)/nLw(555)$, and $nLw(510)/nLw(555)$ in calculating chlorophyll concentration. We also calculated chlorophyll concentrations using the previous SeaWiFS standard algorithm, OC2 [*O'Reilly et al.*, 1998]. OC2 is a simple empirical bio-optical algorithm
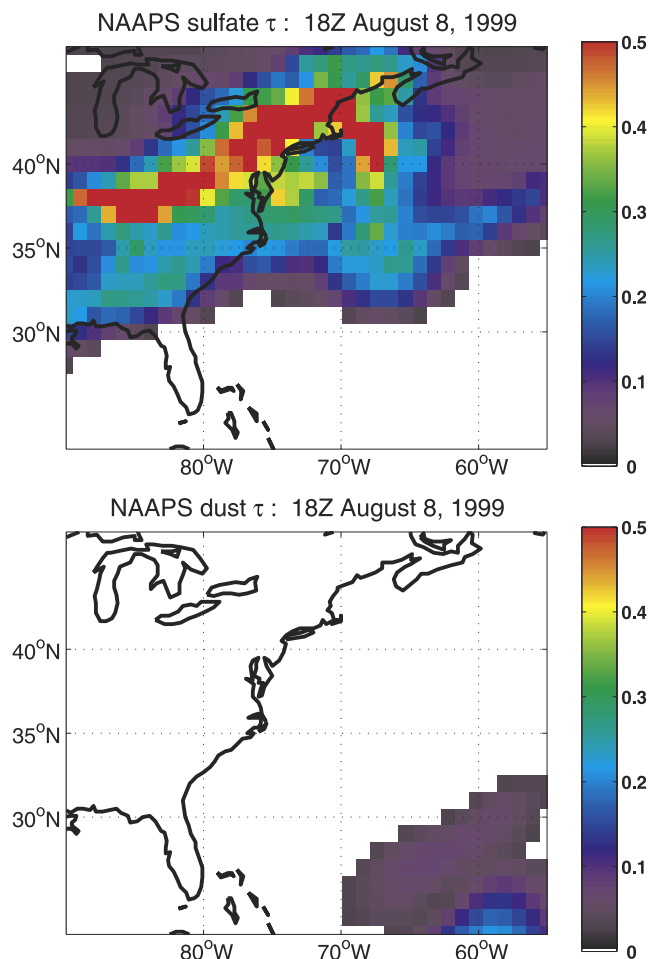

Figure 5. NAAPS aerosol optical thickness (τ) for 8 August 1999: (top) sulfate and (bottom) dust.
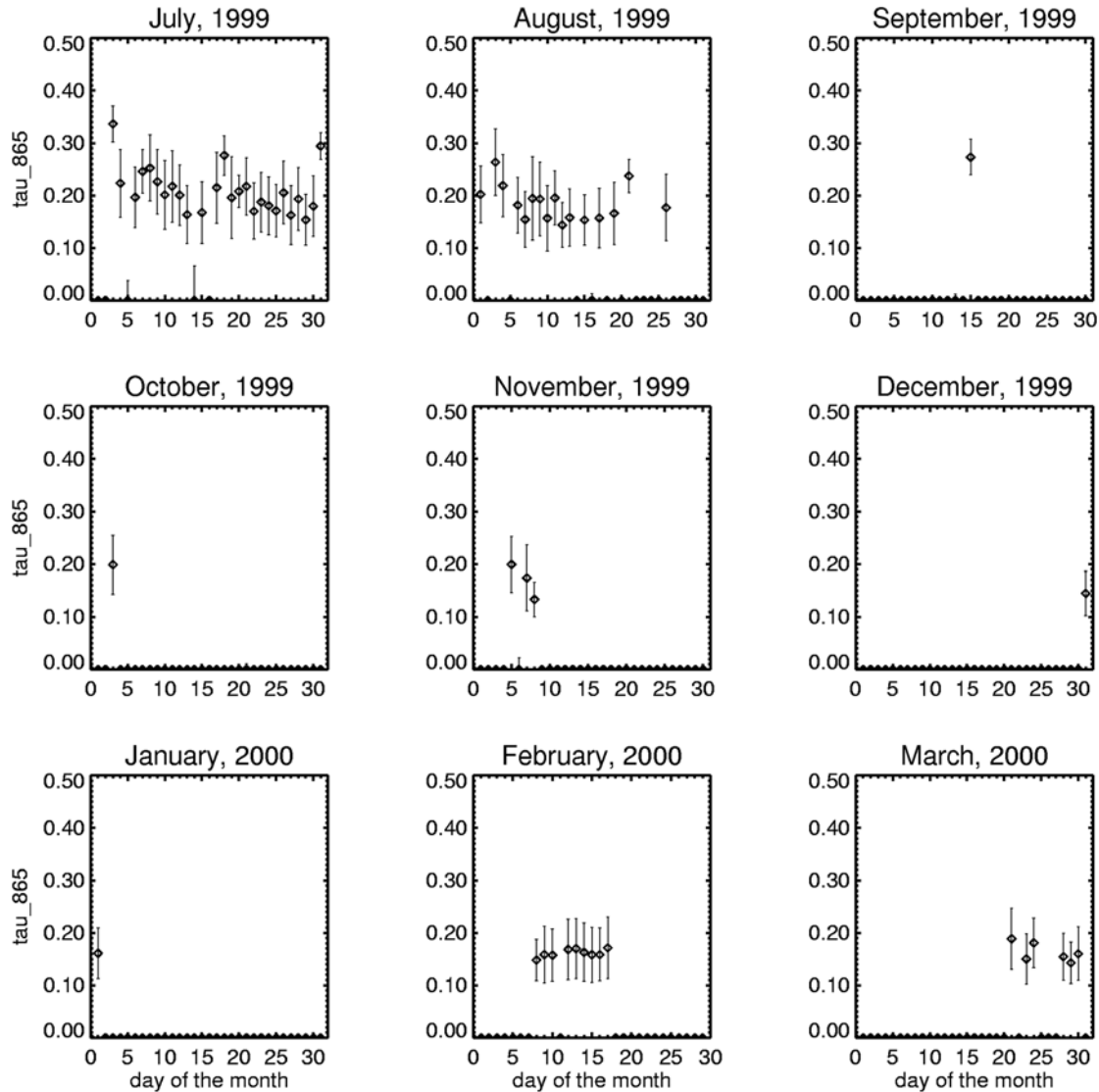
Figure 6. Mean SeaWiFS tau-865 for daily dust dominant pixels in the Sargasso region. Error bars indicate first standard deviation. Zero values indicate either no SeaWiFS coverage in the region or no dust dominant pixels.

that estimates chlorophyll concentration using the logarithm of the $nLw(490)/nLw(555)$ band ratio. In general, OC4 yielded lower chlorophyll estimates, compared more favorably with the in situ reference data, and resulted in more samples for the chl_{lowest} range of this study.

[8] Clear-sky monthly composites were generated by including all pixels whose tau-865 value was less than 0.05. We then calculated the geometric mean of chlorophyll a and the five nLw bands. Within the Sargasso Sea region we used SeaWiFS-derived chlorophyll values to segregate two low-chlorophyll categories on a scene-by-scene basis: chl_{low} includes concentrations between 0.06 and 0.13 mg m^{-3}; chl_{lowest} are concentrations less than 0.06 mg m^{-3}. The clear-sky chl_{lowest} pixels were used to generate monthly average nLw spectra (Figure 3), which demonstrate a slight seasonal variation, although it is suppressed because of the limited range of chlorophyll values included. The summertime spectra are the bluest, with the maximum in

August, which is also the month of minimum chlorophyll (0.03 mg m^{-3}). The wintertime spectra are less blue, with the minimum in December, while the chlorophyll maximum for these months and pixels occurs in January (0.05 mg m^{-3}). Assuming that the sensor is calibrated correctly at the wavelengths used by OC4, the slight offset between the seasonal variation in the clear-sky blue water spectra and the chlorophyll maximum and minimum suggests that the nLw spectrum in the Sargasso Sea is not simply a function of chlorophyll a concentration. We selected the 122 Sea-BAM data points, which fit into our chl_{lowest} classification and plotted the resulting average SeaBAM spectrum against the SeaWiFS monthly averages for August and December 1999 (Figure 4). The SeaWiFS clear-sky December average falls within one standard deviation of the SeaBAM average at 443/555, but the SeaWiFS August average is closer at 490/555, and both months are outside one standard deviation at 510/555. Monthly average clear-sky spectra for the
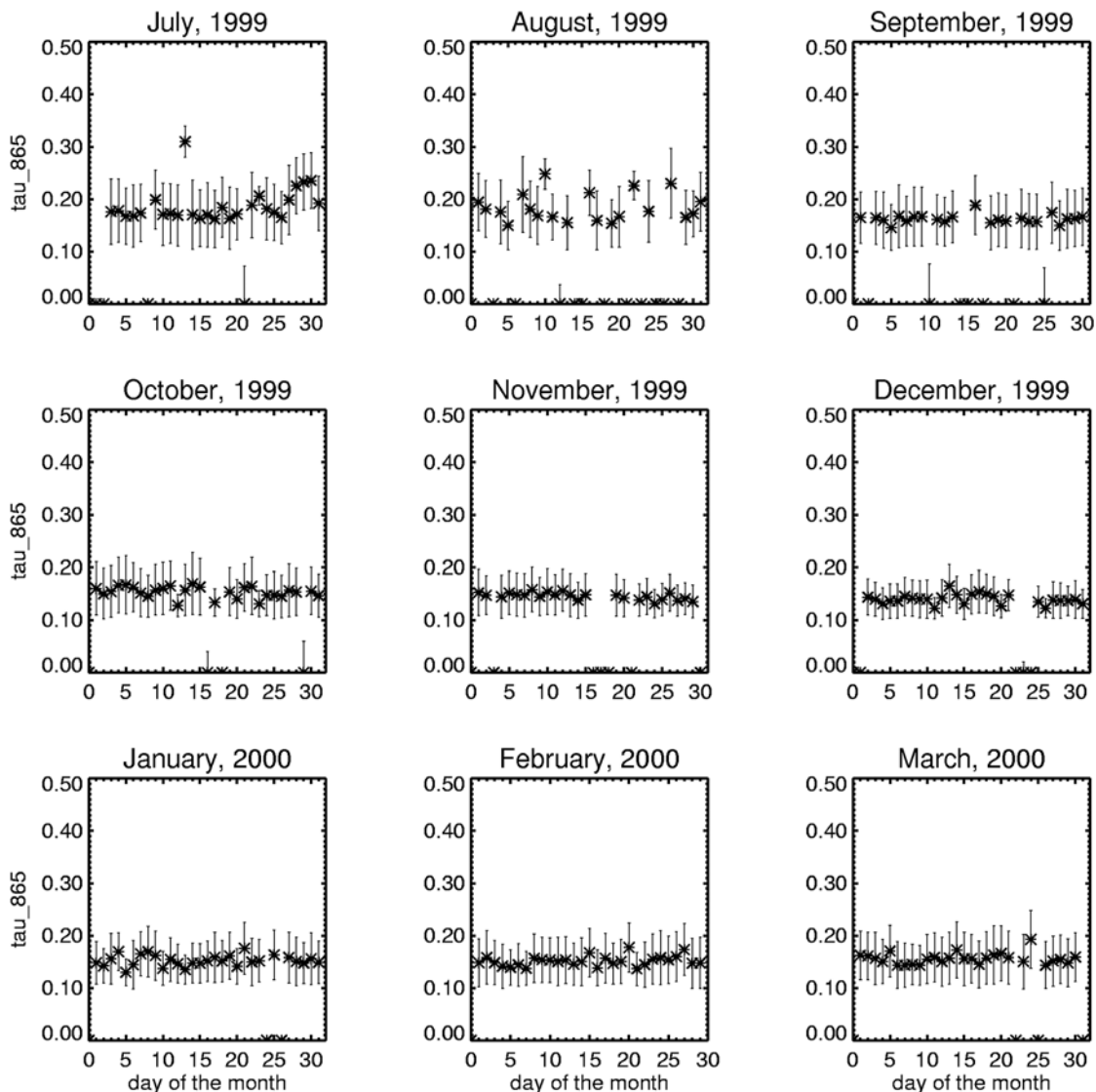
Figure 7. Mean SeaWiFS tau-865 for daily sulfate dominant pixels in the Sargasso region. Error bars indicate first standard deviation. Zero values indicate either no SeaWiFS coverage in the region or no sulfate dominant pixels.

Sargasso Sea are used as the reference in comparison with the aerosol loading cases.

2.2. NAAPS Aerosol Species Information

[9] NAAPS predicts the global distribution of sulfate, dust, and smoke aerosols. The model has been operating continuously since March 1999 at the Naval Research Laboratory, Monterey, California (http://www.nrlmry.navy.mil/aerosol). This global aerosol model is a modified form of the Northern Hemisphere model developed by *Christensen* [1997]. The meteorological fields are provided by the Navy Oceanographic Global Analysis Prediction System [*Hogan and Rosmond*, 1991; *Hogan and Brody*, 1993]. The NAAPS model analyzes the global distribution of tropospheric aerosols on a 1×1 degree grid at 6 hour intervals and 18 vertical levels. The 18Z synoptic time NAAPS aerosol optical depths (τ) at 550 nm are closest to the SeaWiFS east coast pass and were used in this study. Examples of NAAPS τ fields are plotted in Figure 5.

Presently incorporated in this model are sulfur emissions from industrial sources, based on the Global Emissions Inventory Activity [*Benkovitz et al.*, 1996]. Oceanic dimethyl sulfide production is included in the model as a function of season only. For dust, erodibility is based on the U.S. Geological Survey Land Cover Characteristics Database (deserts, salt playas, and sparse dunes and ridges are presumed dust-producing land types) as well as Total Ozone Mapping Spectrometer (TOMS) data. Dust emission occurs whenever the friction velocity exceeds a threshold value and the surface moisture is less than a critical value. Smoke was incorporated into the model beginning in August 1999 for a limited number of source regions in South and Central America, Africa, and Australia. The model never showed smoke off the U.S. east coast during the study period.

[10] We used the NAAPS aerosol model to determine the dominant aerosol species when the SeaWiFS tau-865 was greater than or equal to 0.1: pixels dominated by sulfate
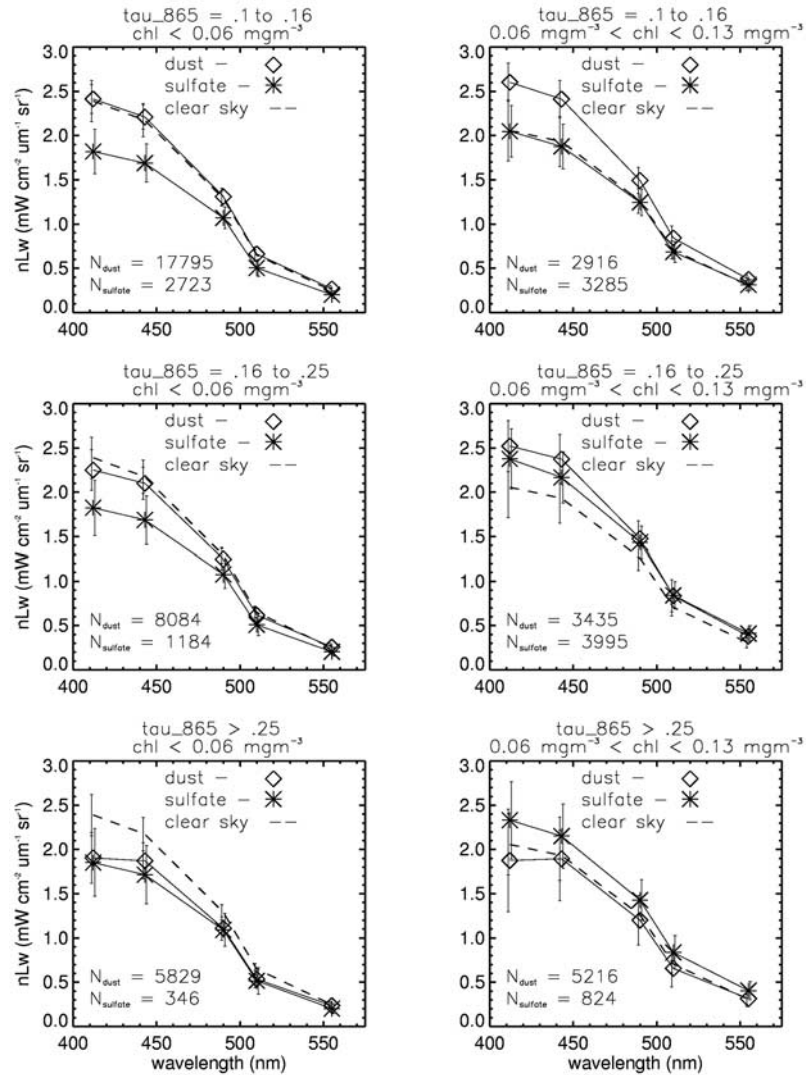
Figure 8. For 8 August 1999: mean clear-sky average SeaWiFS $nLw(\lambda)$ spectra for August (dashed line) with error bars indicating the first standard deviation versus dust dominant average spectra (diamonds) and sulfate dominant average spectra (asterisks) plotted for (left) chl_{lowest} pixels and (right) chl_{low} pixels with tau-865 (top) between 0.1 and 0.16; (middle) tau-865 between 0.16 and 0.25; and (bottom) tau-865 greater than 0.25.

aerosols were defined as those for which NAAPS sulfate τ was greater than 70% of the total aerosol load; pixels dominated by dust aerosols were defined as dust τ greater than 70% of the total aerosol load; and clear pixels were defined as those for which tau-865 was less than 0.05 and both sulfate τ and dust τ less than 0.05. For scenes between March 1999 and March 2000 in which any of the three aerosol cases was dominant, nLw spectra for the low-chlorophyll pixels in the scene were compared to that month's average clear-sky nLw spectrum.

3. Results and Discussion

3.1. Distribution of Aerosol Events

[11] Dust events were episodic but reached the Sargasso with greatest frequency and magnitude during July and August as the time series between July 1999 and March

2000 shows (Figure 6). During summer, when the Sargasso is typically under the Bermuda-Azores high-pressure system, dust was transported from Africa in the Easterly trades, resulting in regional average tau-865 values occasionally greater than 0.3. During at least 17 days during the summer of 1999, air samples taken at Miami confirmed filtered dust was of Saharan origin (J. M. Prospero, personal communication, 1999). During other months, dust events from Africa infrequently reached the Sargasso (in November, January, February, and March). Both during 1999 and 2000, there were late March/early April dust events from the west, which may have traveled from as far away as Asia.

[12] Sulfate was nearly ubiquitous off the U.S. east coast, as the time series from July 1999 through March 2000 in Figure 7 shows. Sulfate was at a maximum during summer with associated average tau-865 values over the Sargasso around 0.2 during June/July. Sulfate levels gradually de-
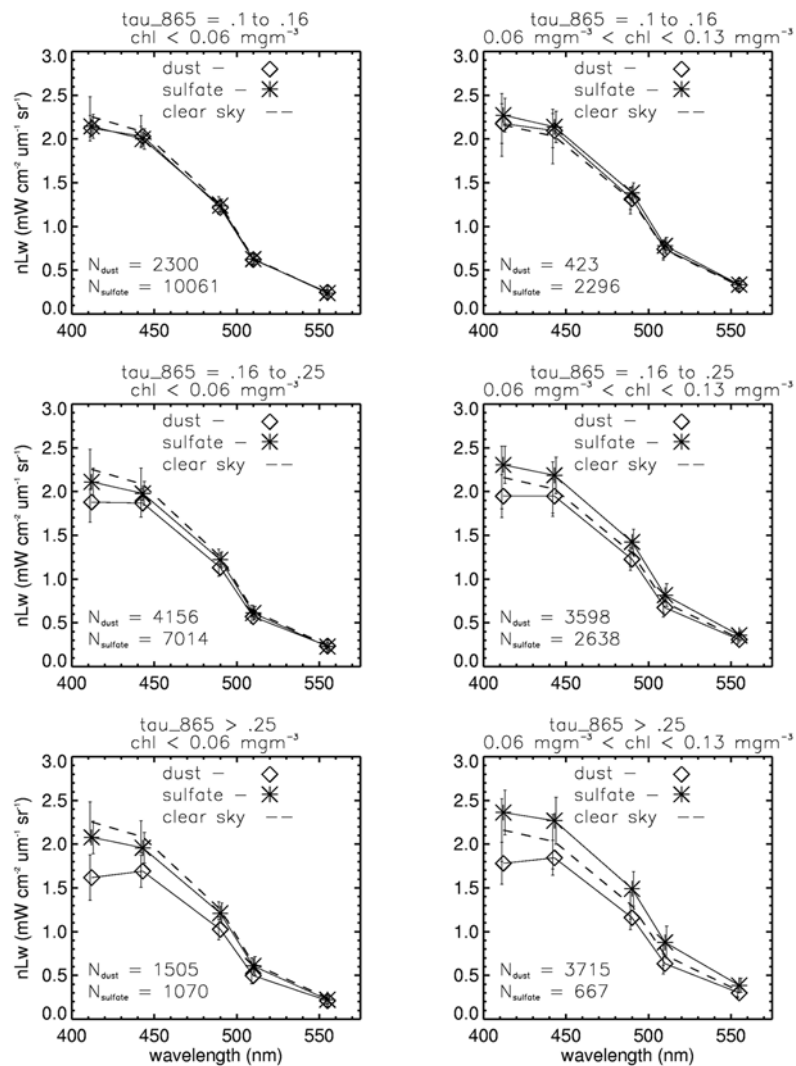
Figure 9. For 9 July 1999: mean clear-sky average SeaWiFS $nLw(\lambda)$ spectra for July (dashed line) with error bars indicating the first standard deviation versus dust dominant average spectra (diamonds) and sulfate dominant average spectra (asterisks) plotted for (left) chl_{lowest} pixels and (right) chl_{low} pixels with (top) tau-865 between 0.1 and 0.16; (middle) tau-865 between 0.16 and 0.25 and (bottom) tau-865 greater than 0.25.

creased to average tau-865 around 0.15 during winter (November through January).

3.2. Comparisons of SeaWiFS Spectra During Dust Events

[13]   The numerous summertime dust events were associated with $nLw(\lambda)$ decreasing at the blue wavelengths as tau-865 increased in comparison to the clear-sky average spectra for the month (Figures 8 and 9). By contrast, the $nLw(555)$ retrievals were mostly unaffected by increasing dust. The result was decrease of the band ratios used in the chlorophyll a algorithms yielding elevated concentrations. Chlorophyll a estimates were typically more than 50% higher for the pixels under the heaviest dust load ($0.25 <$ tau-865 < 0.3) compared to the days immediately preceding and following the dust episode. For example, the dust event between 7 and 10 July was associated with chlorophyll a values around 0.072 mg m^{-3}, compared to an average of 0.048 mg m^{-3} for

the same pixels 3 days earlier and 0.049 mg m^{-3} 3 days later. For the dust event from 23 to 27 July, chlorophyll a values jumped to 0.073 mg m^{-3} compared to 0.045 mg m^{-3} before and 0.047 mg m^{-3} after the dust episode. Between 6 and 10 August, chlorophyll a values associated with a dust event were 0.067 mg m^{-3} compared to 0.044 mg m^{-3} before and 0.046 mg m^{-3} after the dust episode.

[14]   A few dust events during late winter/early spring came from different directions. In February and March 2000, dust of apparent Saharan origin entered the region via a northerly route, instead of from the typical summertime route from the southeast. While these events are more difficult to separate from the sulfate events so common in the northern Sargasso, the effect of the dust upon the nLw spectra and chlorophyll a estimates seems to be the same as during the summer, with chlorophyll concentration values at least 30% higher during the event than immediately before and after the dust was present. Toward the end of March, both in 1999 and 2000,
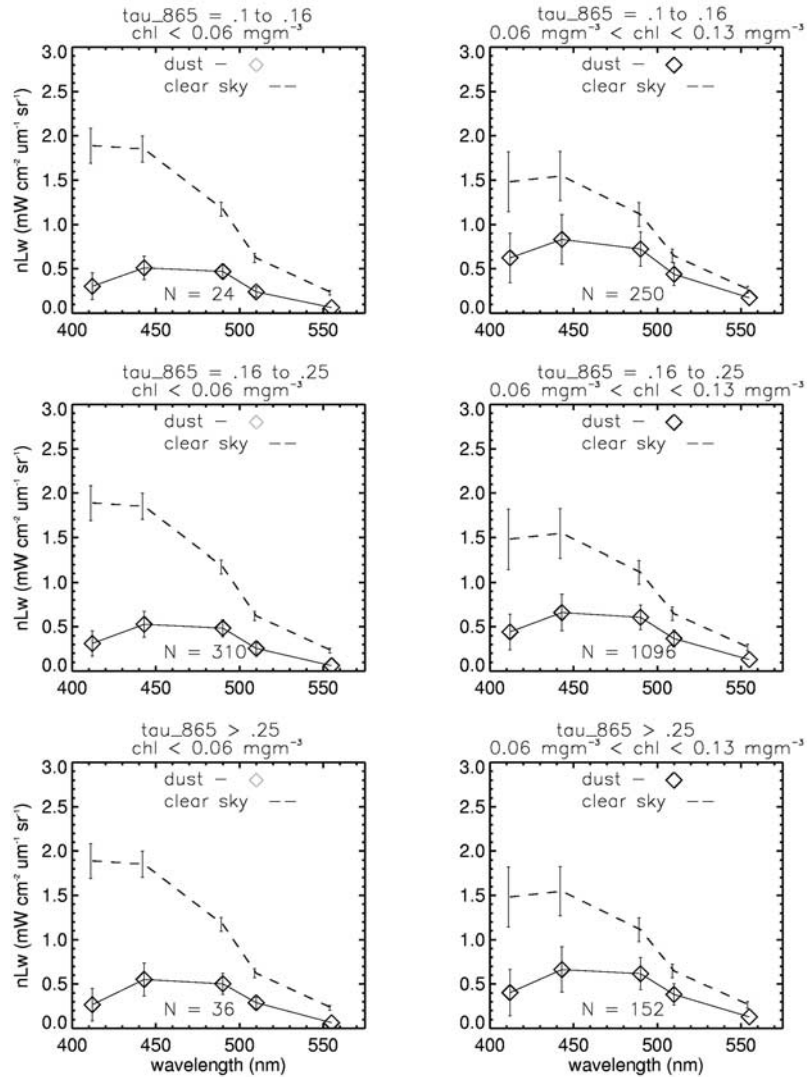
Figure 10. For 31 March 1999: mean clear-sky average SeaWiFS $nLw(\lambda)$ spectra for March (dashed line) with error bars indicating the first standard deviation versus dust dominant average spectra (diamonds) plotted for (left) chl_{lowest} pixels and (right) chl_{low} pixels with (top) tau-865 between 0.1 and 0.16; (middle) tau-865 between 0.16 and 0.25; and (bottom) tau-865 greater than 0.25.

there was an unusual dust episode that approached from the west, possibly originating in Asia as indicated in the NAAPS fields but as yet unconfirmed because of the lack of in situ samples. The effect of these dust events upon the retrieved nLw spectra is pronounced: the nLw spectra are significantly depressed from the clear-sky monthly average across the entire visible spectrum, including 555 nm, for both chlorophyll categories and tau-865 ranges (Figure 10). Despite the decreases in both blue and $nLw(555)$ retrievals the net effect was a lowering of the band ratios and artificially higher chlorophylls; for example, one area experienced a doubling in concentrations from values around 0.05 mg m^{-3} to values greater than 0.1 mg m^{-3}.

3.3. Comparisons of SeaWiFS Spectra During Sulfate Events

[15] For the Sargasso region we found that increasing amounts of sulfate generally correspond to increasing nLw

at all bands, including 555 nm. Since the increase at 555 nm was proportionally greater than the increase at lower wavelengths, both 443/555 and 490/555 band ratios decreased and chlorophyll a estimates increased. This effect is particularly evident at chl_{low} concentrations (Figures 8 and 9). Because we bin the data by chlorophyll amounts on a scene-by-scene basis, the atmospheric contamination that biases the chlorophyll values high skews the affected pixels toward the chl_{low} category. Therefore the chl_{lowest} bins are less indicative of the aerosol loading problem.

[16] During the sulfate event over the northern Sargasso between 8 and 12 August, chlorophyll a concentrations increased more than 60% to 0.091 mg m^{-3} compared to 0.056 mg m^{-3} during the 4 days before and after the sulfate was present. Such increases were typical whenever large amounts of sulfate migrated over the region. Examination of the nLw spectra and chlorophyll concentrations for the same pixels before and after sulfate loading strongly suggests that
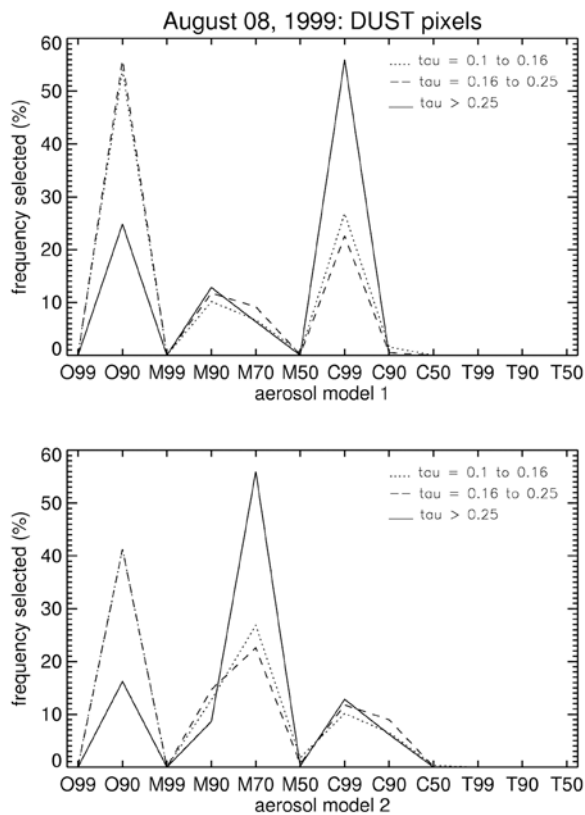
Figure 11. For 8 August 1999: aerosol model pairs used in standard SeaWiFS processing for Sargasso dust dominant chl$_{low}$ pixels plotted by model type (O, oceanic; M, maritime; C, coastal; and T, tropospheric. Number indicates % relative humidities) and frequency selected plotted for tau-865 between 0.1 and 0.16 (dotted line); for tau-865 between 0.16 and 0.25 (dashed line); and for tau-865 greater than 0.25 (solid line). Aerosol models along the horizontal axis are ordered with increasing spectral slope to the right.

chlorophyll concentrations were artificially elevated owing to incorrect atmospheric correction.

3.4. Aerosol Models Within SeaWiFS Atmospheric Correction

[17] The variation in the *nLw* spectra for these low-chlorophyll Sargasso waters appears to be caused by inadequate atmospheric correction. Either the wrong aerosol models are being applied within SeaDAS, or none of the 12 aerosol models in the SeaWiFS atmospheric correction scheme is adequate for some of the aerosol scenarios found off the U.S. east coast. There is currently no method to measure the absorption characteristics of aerosols from satellite [*Gordon and Voss*, 1999]. For strongly absorbing aerosols, information about the aerosol vertical distribution (layer thickness) is required for adequate retrieval and correction. It has been suggested that absorbing aerosols in the Atlantic are mixed higher in the atmosphere than assumed in the existing SeaWiFS candidate aerosol model lookup tables [*Gordon*, 1997].

[18] The 12 aerosol models in the SeaWiFS atmospheric correction are based on models developed by *Shettle and*

Fenn [1979] for LOWTRAN. According to *Gordon* [1997], at 550 nm the tropospheric model has refractive indices ranging from $1.53-0.0066i$ at 0% relative humidity (RH) to $1.369-0.0012i$ at 98% RH, including some absorption (single-scattering albedo between 0.96 and 0.99 for RH between 0 and 98%) and assumes diameters less than 0.1 μm. The oceanic model has no absorption (single-scattering albedo = 1), with refractive indices ranging from 1.5 at 0% RH to 1.35 at 98% RH, and assumes diameters between 0.3 and 1.2 μm for RH between 0 and 98%. The other two SeaWiFS aerosol models are a combination of these: maritime model is 99% tropospheric and 1% oceanic-, and coastal model is 99.5% tropospheric and 0.5% oceanic [*Gordon*, 1997]. Thus none of the models simulate strongly absorbing aerosols well. Furthermore, if dust particles have diameters larger than 0.1 μm, the single-scattering albedo would be lower than that assumed by the SeaWiFS aerosol models since larger dust particles are more absorbing than smaller particles [*Tegen et al.*, 1996. For example, at 550 nm, smaller particles (radius of 0.1 μm) have single-scattering albedo around 0.96, compared to larger particles (radius of 1 μm) with single-scattering albedo around 0.89. For a fixed particle size, maritime aerosols are less absorbing at blue wavelengths than at near-infrared wavelengths [*Lenoble*, 1993], while soot is more absorbing at the blue wavelengths than at near infrared. When absorbing aerosols are present, the success of the atmospheric correction depends upon the selection of an aerosol model that incorporates absorption. Since dust and soot are especially absorbing at blue wavelengths, but much less so at the near-infrared bands from which the aerosol models are selected, the aerosol model selected is likely to be one that does not account for enough absorption, such as an oceanic or maritime model. Additionally, if either the size or type of particle or the relative humidity were different from that assumed by the SeaWiFS models, an incorrect atmospheric correction would result.

3.4.1. Aerosol Model Performance on Pixels Dominated by Dust

[19] For the pixels dominated by dust aerosols in the 8 August scene for chl$_{low}$ concentrations the oceanic-90 model was selected with greatest frequency for lower tau-865 amounts (Figure 11). With increasing tau-865 the maritime and coastal models were selected more often, resulting in a SeaWiFS atmospheric correction that had more spectral variation, attributing relatively more aerosol radiance at the blue end of the spectrum. Since the tropospheric models include the most absorption of all the aerosol models, it is interesting to note that SeaDAS never selected them for these dust pixels. A possible explanation for the difference between the 8 August pixels dominated by dust aerosols and the clear-sky monthly average spectra (Figure 8) is that the atmospheric correction often did not factor in enough absorption at low tau, particularly for chl$_{low}$, and selected an aerosol model with too much absorption at high tau, which resulted in an atmospheric overcorrection with too much of the total top-of-the-atmosphere radiance being attributed to aerosols, particularly for the chl$_{lowest}$ pixels. At low tau a slightly absorbing aerosol model would have probably been appropriate (e.g., maritime or coastal), while at higher tau, slightly less absorbing models would have been more suitable (e.g., maritime).
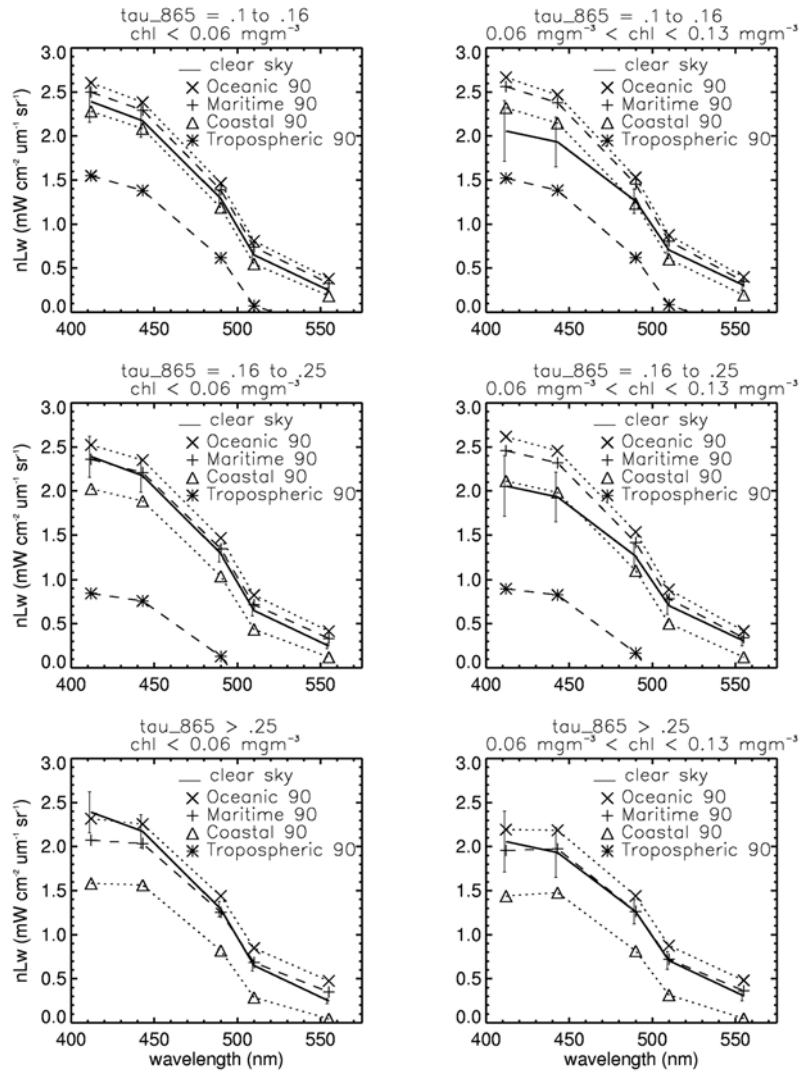
Figure 12.   For 8 August 1999: SeaWiFS fixed aerosol model runs versus clear-sky monthly average for dust dominant pixels in the Sargasso plotted for (left) chl$_{lowest}$ pixels and (right) chl$_{low}$ pixels (top) for tau-865 between 0.1 and 0.16; (middle) for tau-865 between 0.16 and 0.25; and (bottom) for tau-865 greater than 0.25. Note that for the tropospheric 90 run for tau-865 > 0.25 all *nLw*s are negative.

[20]   Fixed aerosol model runs for each of the 12 aerosol models were done to test this idea: the results of four representative models, which span the range of spectral steepness (Figure 2), are shown here along with the clear-sky monthly average spectra (Figure 12). At 555 nm, for all tau-865 and chlorophyll categories the maritime model performed closest to the clear-sky average. For the blue bands the maritime model compared best for half of the categories (generally for higher tau ranges), while the coastal model compared best for lower tau amounts. The tropospheric model was consistently farthest from the clear-sky average, always negative at 555 nm, and performed worse with increasing tau-865, leading to overcorrected or negative *nLw* spectra. Thus the discrepancy between the dust dominant spectra and the clear-sky spectra is not a simple case of neglecting to account for enough absorption. Other possibilities for the incorrect atmospheric correction under dust loading include the coincidence of another aerosol type (e.g., oceanic, typical of desert dust falling into the

marine boundary layer [*Antoine and Morel*, 2000]) or the inability by the SeaWiFS sensor at 865 nm to assess properly dust aerosols, resulting in incorrect extrapolation to lower wavelengths. With increasing tau-865 it is likely that the dust aerosols have either changed particle size distribution, increased relative humidity, or some combination thereof, which has not been properly handled by the aerosol models.

3.4.2.   Aerosol Model Performance on Pixels Dominated by Sulfate

[21]   For the pixels dominated by sulfate aerosols in the 8 August scene (Figure 8) the chl$_{lowest}$ pixels had a fairly consistent atmospheric overcorrection, while the chl$_{low}$ pixels had an increase of *nLw* with increasing tau-865, indicating an atmospheric undercorrection. By itself, sulfate is a nonabsorbing aerosol whose successful atmospheric correction would require an aerosol model that is entirely scattering, such as the oceanic model used within SeaDAS. The chl$_{lowest}$ pixels were likely coincident with sulfate,
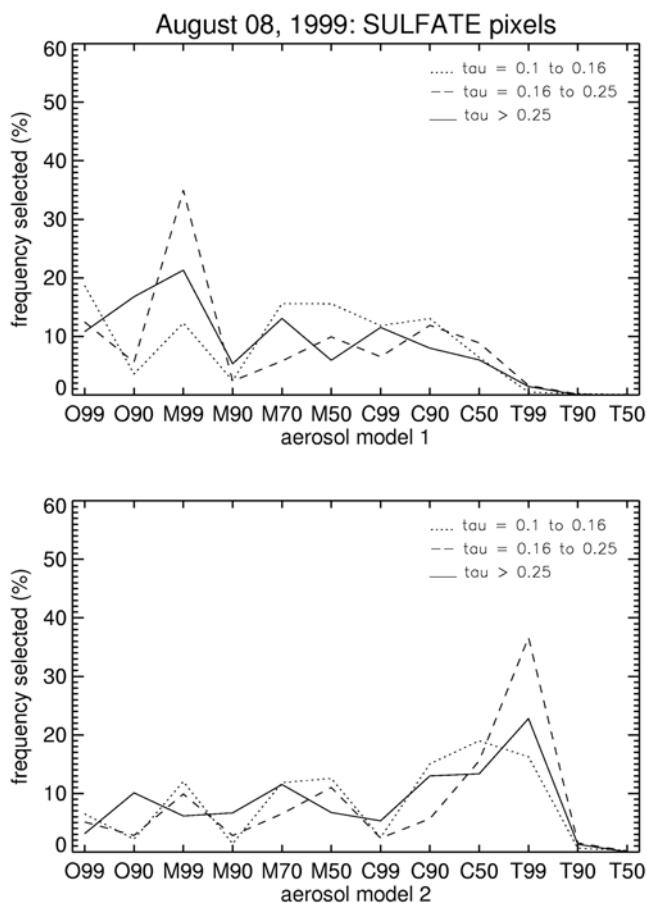
Figure 13. For 8 August 1999: aerosol model pairs used in standard SeaWiFS processing for Sargasso sulfate dominant chl$_{low}$ pixels plotted by model type (O, oceanic; M, maritime; C, coastal; and T, tropospheric. Number indicates percent relative humidities) and frequency selected plotted for tau-865 between 0.1 and 0.16 (dotted line); for tau-865 between 0.16 and 0.25 (dashed line); and for tau-865 greater than 0.25 (solid line). Aerosol models along the horizontal axis are ordered with increasing spectral slope to the right.

which was primarily nonabsorbing, with greater tau corresponding to increasing amounts of sulfate or increasing relative humidity, while the aerosol model applied during atmospheric correction incorrectly assumed some absorption. The sulfate associated with the chl$_{low}$ pixels, however, was either not entirely scattering or had lower relative humidity than assumed. As shown in Figure 13, aerosol model selection for the sulfate pixels did not fit any consistent pattern. For all tau-865 categories, model selection ranged the gamut from oceanic to maritime to coastal and even included high-humidity tropospheric. Since there appeared to be an undercorrection for aerosols in the sulfate dominant pixels as compared to the clear-sky average spectrum, it might be assumed that more absorption or less relative humidity was present than the models assumed. Fixed model runs for each of the 12 aerosol models were done on this scene for the pixels dominated by sulfate aerosols (Figure 14). At chl$_{lowest}$ concentrations and all ranges of tau-865 the oceanic and maritime models per-

formed the closest to the clear-sky average, confirming that the sulfate population over those pixels was primarily non-absorbing. For chl$_{low}$ pixels the coastal model was the closest to the clear-sky average, confirming the presence of an absorbing aerosol and demonstrating that a lower relative humidity model would have been more successful still with increasing tau. Again, the tropospheric model yielded consistently negative nLw(555) retrievals, but the model performed more respectably at blue wavelengths than it did for the dust dominant pixels. These results suggest the coexistence of sulfate with some absorbing aerosols such as black carbon and soot, which has been observed during field experiments to be an important component of the mid-Atlantic haze plume, with the carbonaceous fraction increasing with increasing height [*Russell et al.*, 1999]. Clearly the sulfate population off the U.S. east coast is complex and variable. The persistence of this atmospheric feature makes it especially vexing for ocean color satellite remote sensing in this region.

4. Conclusions

[22] There are biases in the SeaWiFS nLw spectra and chlorophyll *a* concentration associated with dust and sulfate events off the U.S. east coast. The current SeaDAS algorithms (Reprocessing Version 3) are an improvement over the previous versions, but we still find persistent discrepancies associated with the two aerosol species discussed here. During the dust events the blue wavelength nLw are typically lowered, leading to overestimation of chlorophyll concentrations on the order of 30–50% higher than the days before and after the dust arrives. During the sulfate events coincident with carbonaceous aerosols the entire spectrum is elevated; the 555 nm band increase is proportionally greater than at the blue wavelengths and causes a decrease in the band ratio going into the chlorophyll algorithm, also resulting in an overestimation of chlorophyll concentrations on the order of 50–70%. Sulfate is particularly problematic for ocean color remote sensing, both because of its greater light scattering potential and its common colocation with black carbon and soot and because it is nearly always present off the U.S. east coast.

[23] Using top-of-the-atmosphere satellite radiance measurements to separate the atmospheric signal from the much smaller water-leaving radiance signal is a difficult problem with no easy alternative at this time. The current arrangement of estimating the aerosol contribution at the near-infrared bands and extrapolating to lower wavelengths using one of 12 aerosol models is prone to error for several reasons, including the difficulty of selecting the correct aerosol model simply from the information at 765 and 865 nm, the situation where the near-infrared bands may be least able to detect the aerosols (i.e., as with dust), and the possibility that there are situations where none of the 12 aerosol models is appropriate, as well as other possible causes. *Gordon and Wang* [1994] suggested that the atmospheric correction could be based upon measured, column-averaged aerosol optical properties to circumvent the reliance on aerosol models. Because these aerosol measurements are required across the spectrum, including visible wavelengths, measurement by satellite alone will not be adequate. Field studies are required to refine aerosol classification techni-
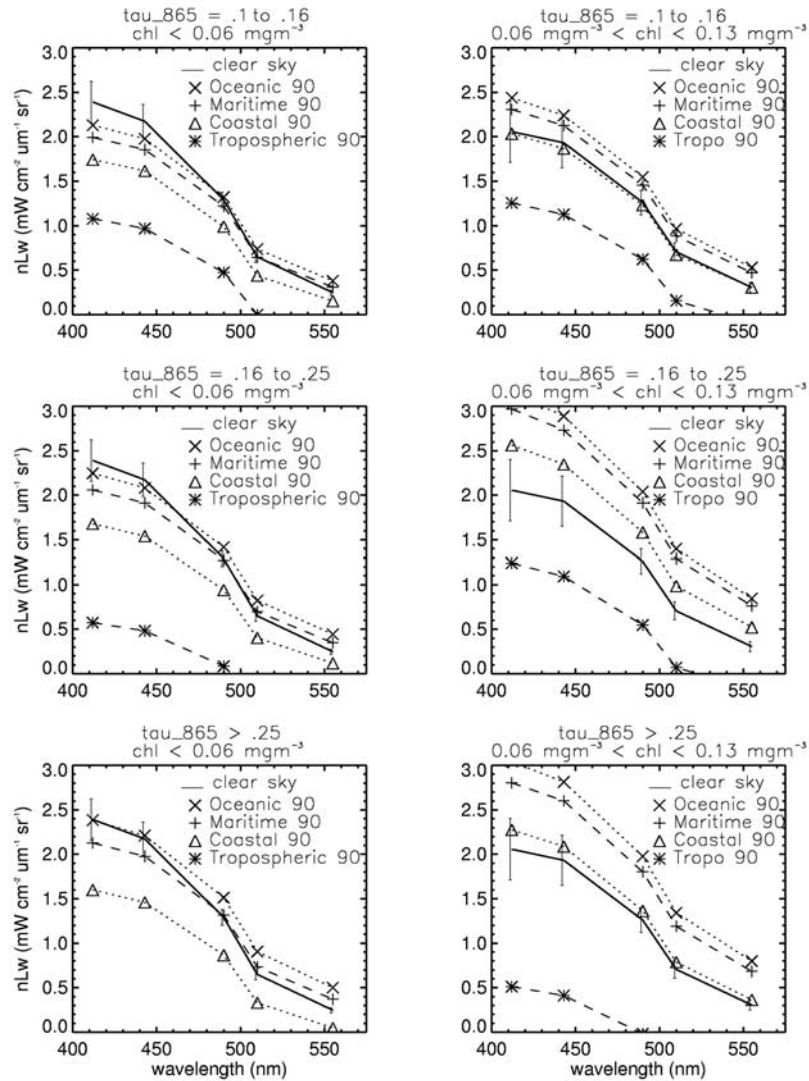
Figure 14. For 8 August 1999: SeaWiFS fixed aerosol model runs versus clear-sky monthly average for sulfate dominant pixels in the Sargasso plotted for (left) chl_{lowest} pixels and (right) chl_{low} pixels (top) for tau-865 between 0.1 and 0.16; (middle) for tau-865 between 0.16 and 0.25; and (bottom) for tau-865 greater than 0.25. Note that for the tropospheric 90 run for tau-865 > 0.25 and chl_{lowest} all nLws are negative.

ques and understand further aerosol optical properties. Ideally, aerosol measurements should be routinely collected by a good network of permanent Sun photometer ground stations, such as the Aerosol Robotic Network (AERO-NET), augmented by observations collected over the oceans by ships and aircraft already reporting routine meteorological observations. A real-time global aerosol model such as NAAPS, which is initialized and closely monitored against in situ data, could be used to fill the remaining data gaps. On the basis of the different behavior of the SeaWiFS spectra associated with the aerosol species discussed here, dust and sulfate, NAAPS is a useful tool for differentiating aerosol populations. In addition to its utility in improving ocean color atmospheric correction, a better understanding of the characteristics of the aerosol population off the U.S. east coast, particularly the presence of dust, sulfate, nitrate, and other anthropogenic pollutants that serve as a potential phytoplankton nutrient source, will enable us to conduct future scientific studies in which we consider the deposition of such aerosols into the ocean and their effect upon the primary productivity of the region.

References

Antoine, D., and A. Morel, Atmospheric correction over the ocean (case I waters), in *MERIS Algorithm Theoretical Basis Document, version 2.7*, Univ. Pierre et Marie Curie et Cent. Natl. de la Rech. Sci., Villefranche sur Mer, France, 2000.

Benkovitz, C. M., M. T. Scholtz, J. Pacyna, L. Tarrason, J. Dignon, E. C. Voldner, P. A. Spiro, J. A. Logan, and T. E. Graedel, Global gridded inventories of anthropogenic emissions of sulfur and nitrogen, *J. Geophys. Res.*, *101*, 29,239–29,253, 1996.

Christensen, J. H., The Danish Eulerian hemispheric model—A three-dimensional air pollution model used for the Arctic, *Atmos. Environ.*, *31*, 4169–4191, 1997.

Fu, G., K. S. Baith, and C. R. McClain, SeaDAS: The SeaWiFS Data Analysis System, paper presented at 4th Pacific Ocean Remote Sensing Conference, PORSEC Admin., Qingdao, China, 1998.

Gordon, H. R., Atmospheric correction of ocean color imagery in the Earth Observing System era, *J. Geophys. Res.*, *102*, 17,081–17,106, 1997.

Gordon, H. R., and A. Y. Morel, *Remote Assessment of Ocean Colour for Interpretation of Satellite Visible Imagery: A Review*, Springer-Verlag, New York, 1983.

Gordon, H. R., and K. J. Voss, *MODIS Normalized Water-leaving Radiance Algorithm Theoretical Basis Document (MOD 18), Version 3*, Univ. of Miami, Coral Gables, Fla., 1999.

Gordon, H. R., and M. Wang, Retrieval of water-leaving radiance and aerosol optical thickness over the oceans with SeaWiFS: A preliminary algorithm, *Appl. Opt.*, *33*, 443–452, 1994.

Hogan, T. F., and L. R. Brody, Sensitivity studies of the Navy's global forecast model parameterizations and evaluation of improvements to NOGAPS, *Mon. Weather Rev.*, *121*, 2373–2395, 1993.

Hogan, T. F., and T. E. Rosmond, The description of the navy operational global atmospheric prediction system's spectral forecast model, *Mon. Weather Rev.*, *119*, 1786–1815, 1991.

Kahru, M., and B. G. Mitchell, Empirical chlorophyll algorithm and preliminary SeaWiFS validation for the California Current, *Int. J. Remote Sens.*, *20*, 3423–3429, 1999.

Lenoble, J., *Atmospheric Radiative Transfer*, A. Deepak, Hampton, Va., 1993.

Li, X., H. Maring, D. Savoie, K. Voss, and J. M. Prospero, Dominance of mineral dust in aerosol light-scattering in the North Atlantic trade winds, *Nature*, *380*, 416–419, 1996.

Morel, A., Optical modeling of the upper ocean in relation to its biogenous matter content (case I waters), *J. Geophys. Res.*, *93*, 10,749–10,768, 1988.

Morel, A., and B. Gentili, Diffuse reflectance of oceanic waters: bidirectional aspects, *Appl. Opt.*, *32*, 6864–6879, 1993.

O'Reilly, J. E., S. Maritorena, B. G. Mitchell, D. A. Siegel, K. L. Carder, S. A. Garver, M. Kahru, and C. McClain, Ocean color chlorophyll algorithms for SeaWiFS, *J. Geophys. Res.*, *103*, 24,937–24,953, 1998.

O'Reilly, J. E., et al., SeaWiFS post-launch calibration and validation analyses, part 3, vol. *11*, edited by S. B. Hooker and E. R. Firestone, *NASA Tech. Memo, 2000-206892*, 49 pp., 2000.

Russell, P. B., P. V. Hobbs, and L. L. Stowe, Aerosol properties and radiative effects in the U.S. east coast haze plume: An overview of the Tropospheric Aerosol Radiative Forcing Observational Experiment (TARFOX), *J. Geophys. Res.*, *104*, 2213–2222, 1999.

Shettle, E. P., and R. W. Fenn, Models for the aerosols of the lower atmosphere and the effects of humidity variations on their optical properties, *AFGL Rep. TR-79-0214*, U.S. Air Force Geophys. Lab., Hanscom Air Force Base, Mass., 1979.

Siegel, D. A., and A. F. Michaels, Quantification of non-algal light attenuation in the Sargasso Sea: Implications for bio-geochemistry and remote sensing, *Deep Sea Res., Part II*, *43*, 321–345, 1996.

Siegel, D. A., M. Wang, S. Maritorena, and W. Robinson, Atmospheric correction of satellite ocean color imagery: The black pixel assumption, *Appl. Opt.*, *39*, 3582–3591, 2000.

Tegen, I., A. A. Lacis, and I. Fung, The influence on climate forcing of mineral aerosols from disturbed soils, *Nature*, *380*, 419–422, 1996.

Wang, M., A sensitivity study of the SeaWiFS atmospheric correction algorithm: Effects of spectral band variations, *Remote Sens. Environ.*, *67*, 348–359, 1999.

—————————

J. E. O'Reilly, Northeast Fisheries Center, Narragansett Laboratory, NOAA/NMFS, Narragansett, RI 02882, USA. (oreilly@fish1.gso.uri.edu)

S. E. Schollaert and J. A. Yoder, Graduate School of Oceanography, University of Rhode Island, Narragansett, RI 02882, USA. (s.schollaert@gso.uri.edu; jyoder@gso.uri.edu)

D. L. Westphal, Marine Meteorology Division, Naval Research Laboratory, 7 Grace Hopper Street, Monterey, CA 93943-5502, USA. (westphal@nrlmry.navy.mil)